

A numerical formulation for electric-mechanical contacts based on microscopic interface laws

Original

A numerical formulation for electric-mechanical contacts based on microscopic interface laws / Boso, D. P.; Zavarise, G.; Schrefler, B. A.. - ELETTRONICO. - (2002), pp. 1-9. (Intervento presentato al convegno GIMC2002 Third Joint Conference of Italian Group of Comput. Mechanics tenutosi a Giulianova, Italy nel 2002).

Availability:

This version is available at: 11583/2700695 since: 2018-04-18T15:04:34Z

Publisher:

AIMETA

Published

DOI:

Terms of use:

This article is made available under terms and conditions as specified in the corresponding bibliographic description in the repository

Publisher copyright

(Article begins on next page)

A NUMERICAL FORMULATION FOR ELECTRIC-MECHANICAL CONTACTS BASED ON MICROSCOPIC INTERFACE LAWS

D. P. BOSO¹, G. ZAVARISE², B.A. SCHREFLER¹

¹ *Dipartimento di Costruzioni e Trasporti, Università di Padova, Padova*

boso@caronte.dic.unipd.it bas@caronte.dic.unipd.it

² *Dipartimento di Ingegneria Strutturale e Geotecnica Politecnico di Torino, Torino*
zavarise@athena.polito.it

ABSTRACT

This work is devoted to the development of a new constitutive model for electric–mechanical contacts, based on a micro-macro approach to describe the contact behaviour.

In order to model properly the physical aspect of the problem the surface microrugosity must be considered. In the proposed contact element a macroscopic formulation, based on microscopic evidences, is set up and implemented in the contact formulation.

Some thermo-mechanical macroscopic models, based on microscopic characterizations, have already been developed to compute the normal and tangential contact stiffness and the thermal contact resistance. On the basis of such macroscopic models, a similar model, suitable for the electric-mechanical field, is developed. With reference to the thermal constriction resistance the electric contact resistance is studied, assuming a flux tube around each contacting asperity, and choosing a suitable geometry for its narrowing at the contact zone.

Finally these selected microscopic laws are adapted to the macroscopic numerical necessities to obtain a constitutive law for the electric-mechanical contact element.

Consistent linearization is developed in order to improve the computational speed, within the framework of the implicit methods.

1. INTRODUCTION

Within the Finite Element framework the numerical treatment of contact problems is generally based on two main solution strategies, i.e. the Lagrange multipliers method and the penalty method. Usually in both cases the physical behaviour of the contacting surfaces is not taken into account. In the case of the Lagrange multipliers technique the non-penetration conditions are satisfied exactly, but they are purely geometrical constraints and any physical aspect of the contact is disregarded. Considering the penalty method, the penalty parameter is usually chosen on the basis of numerical necessities. It is well known that a wrong choice of the parameter can lead to the ill-conditioning of the global stiffness matrix or to an

unacceptable violation of the contact constraints. However penalty methods can be easily implemented in the structure of the Finite Element codes, so that they are widely used.

Actually within the framework of the penalty method it is possible to implement contact elements with interfacial constitutive laws, thus overcoming their limitation of being a pure solution strategy.

In the present paper this possibility is exploited to develop a new contact element suitably formulated to deal with contact problems in the coupled electric and mechanical fields. In the formulation the real physical mechanisms of contacting surfaces is taken into account using a non-linear constitutive relationship. The basic concept of contact as a unilateral constraint condition is extended through the implementation of a suitable constitutive law that describes at macroscopic scale what happens on the microscopic one. In this way the physical contact behaviour is determined using micro-mechanical formulations to develop a constitutive law for the contact finite element.

2. CONTACT CONSTITUTIVE LAWS

2.1. Surface parameters characterization and normal contact contribution

When two surfaces come into contact the real contact area is actually concentrated on the summits of the highest asperities, hence it is composed of a collection of spots.

The determination of the true contact area is fundamental for an accurate modelling of mechanical and electric phenomena; this means that it is necessary to determine the number of spots, their distribution and their medium size. All these parameters depend upon the applied contact pressure. The problem can be approached using either correlation formulae generated by fitting a set of experimental results or via a theoretical analysis.

In this study a microscopic plastic model [1] afterwards enhanced [2-5], has been preferred and suitably adapted. The model was originally developed for the thermo-mechanical field, but in two recent works [6-7] we proposed the approach for the electric-mechanical one. This paper is the further development of that approach and for self-consistency we recall here the main lines of that study. The statistic characterization of the contacting surfaces proposed in [1] is used to determine the number of spots per unit area n_{sc} and their mean spot radius \bar{a}

$$n_{sc} = \frac{N_{sc}}{A_a} = \frac{1}{16} \cdot \frac{\bar{m}^2}{\sigma^2} \cdot \frac{\exp\left(-\frac{d^2}{\sigma^2}\right)}{\operatorname{erfc}(d/\sqrt{2}\sigma)} \quad (1)$$

$$\bar{a} = \sqrt{\frac{8}{\pi}} \cdot \frac{\sigma}{\bar{m}} \cdot \exp\left(\frac{d^2}{2 \cdot \sigma^2}\right) \cdot \operatorname{erfc}\left(\frac{d}{\sqrt{2}\sigma}\right) \quad (2)$$

where A_a is the apparent contact area, d is the mean planes distance, \bar{m} is the mean absolute asperity slope and σ is the RMS surface roughness.

Combining equations (1) and (2) the ratio between the real and the apparent contact area can be expressed in the form

$$\frac{A_r}{A_a} = n_{sc} \pi \bar{a}^2 = \frac{1}{2} \operatorname{erfc}\left(\frac{d}{\sqrt{2}\sigma}\right) \quad (3)$$

In the usual range of applied pressures the parameters \bar{m} and σ can be kept constant, so that only the mean planes distance governs the evolution of the number of spots and their mean radius. In order to predict the contact conductance a mechanical dependence is introduced to relate the pressure applied at the interface to the real contact area A_r , or to the ratio A_r/A_a . This model is developed assuming that the local contact pressure is high enough to induce plasticisation on the top of the asperities, even for low apparent contact pressures. With such assumption the real contact pressure in the contact zones reaches the yielding value and the following relationship holds

$$A_r H = A_a p = F \quad (4)$$

where H is the asperities yielding limit, p is the apparent pressure and F is the total contact force. The proportionality parameter H plays a key role in the models of plastic type. It represents the surface hardness, which is completely different from that of the bulk material. Hardening processes usually occur on the external stratum, due to finishing treatments, contaminants, oxidation and other causes. Hence the effective yield pressure (which can be determined using micro-hardness tests) depends upon the depth of the plastic zone and its value can vary within a wide range.

The results of Vickers micro-hardness tests can be correlated in a power form [8]

$$H_V = c_1 \cdot d_v^{c_2} \quad (5)$$

where H_V is Vickers micro-hardness in MPa, d_v is the mean indenter diagonal and c_1, c_2 are the correlation coefficients depending upon the material.

Assuming that the contact micro hardness of the surface being penetrated by the asperities of the harder surface is the same as the Vickers indentation we have

$$d_V = \sqrt{2\pi} 10^6 \bar{a} \quad (6)$$

where the 10^6 factor has been introduced to use meter as length unit.

In this way Vickers micro-hardness can be related to the relative mean planes distance through eqs. (2), (5) and (6)

$$H_v = c_1 \left[4 \cdot 10^6 \frac{\sigma}{\bar{m}} \exp\left(\frac{d^2}{2\sigma^2}\right) \operatorname{erfc}\left(\frac{d}{\sqrt{2}\sigma}\right) \right]^{c_2} \quad (7)$$

Equations (7) and (3) through (4) can be combined to obtain the following relationship between the apparent contact pressure p and the mean planes distance d

$$p = c_1 \left[4 \cdot 10^6 \frac{\sigma}{\bar{m}} \exp\left(\frac{d^2}{2\sigma^2}\right) \operatorname{erfc}\left(\frac{d}{\sqrt{2}\sigma}\right) \right]^{c_2} \cdot \frac{1}{2} \operatorname{erfc}\left(\frac{d}{\sqrt{2}\sigma}\right) \quad (8)$$

It is worth to mention that the inverse complementary error function $\operatorname{erfc}(d/\sqrt{2}\sigma)$, appearing in the above equations, has not solution in closed form, hence numerical integration is needed.

2.2. Electric Contact Resistance

Different techniques for the computation of the electric contact resistance, taking into account the dependences on various parameters, have been proposed. Just like the mechanical field, some of the available laws are obtained as a curve fitting of experimental results, while others are developed on theoretical basis.

Considering the phenomena at microscopic level, the resistance is mainly due to the low fraction of surface area really in contact, which causes the main perturbation of the electric field in the interface zones. Electric resistance is calculated assuming that each single spot contribution can be added in parallel to the others, thus obtaining the resistance over the apparent contact area. The electric constriction resistance is studied supposing a flux tube around each asperity in contact, and choosing a suitable geometry for its narrowing at the contact zone. Various kinds of narrowing have been studied and comparisons with experimental tests show the best correspondence for the flat disk narrowing model. In the case of a disk and a half space it gives the following constriction resistance [9]

$$R_i = \frac{1}{4k^* a} \quad (9)$$

where k^* is the mean harmonic conductivity of the joint if two different materials are in contact, $k^* = (2k_1 k_2)/(k_1 + k_2)$. To deal with a flux tube the conductance is half the previous one, and a correction rule, ψ_i , as a function of the narrowing radius a_i and the flux radius b_i must be applied

$$c_{V_i} = \frac{2k^* a_i}{\psi_i} = \frac{2k^* a_i}{(1 - a_i/b_i)^{1.5}} \quad (10)$$

Applying this result to each ideal tube the total conductance of the joint is

$$h_V = \frac{I/A_a}{\Delta V} = \frac{2k^*}{A_a} \sum \frac{a_i}{\psi_i} = \frac{2k^*}{A_a \psi} \sum a_i \quad (11)$$

and by recalling eq. (1), (2) and (3), after some algebra

$$h_V = \frac{k^* \bar{m}}{2\sigma} \left(1 - \sqrt{\frac{p}{H}}\right)^{-1.5} \frac{\exp(-d^2/(2\sigma^2))}{\sqrt{2\pi}} \quad (12)$$

3. FINITE ELEMENT FORMULATION

3.1. Contact element geometry

The present geometrical formulation is based on an enhanced version of the well-known node-to-segment contact element proposed by Wriggers and Simo [10]. Some new geometrical variables are introduced to improve the correspondence between the geometric description and the physical formulation. Here we recall the main geometrical parameters defining the element behaviour, i.e. the normal gap g_N , the voltage jump g_V and the contact area. Interested readers can find all the details on geometrical relationships and their linearization in [11-12]. The model is here discussed for two-dimension problems, the extension to a three-dimension analysis has only formal complications, but not conceptual difficulties. For the sake of simplicity in the algorithm formulation it is assumed that contact surfaces can be described by 2D linear isoparametric elements.

With reference to Figure 1 the normal gap g_N is computed nodalwise, measuring the distance between the slave node S and its projection onto the master segment

$$g_N = (\mathbf{x}_S - \mathbf{x}_1) \cdot \mathbf{n} \quad (13)$$

where \mathbf{n} is the unit vector perpendicular to the master segment 1-2, \mathbf{x}_S and \mathbf{x}_1 are vectors identifying the current position of nodes S and 1 respectively.

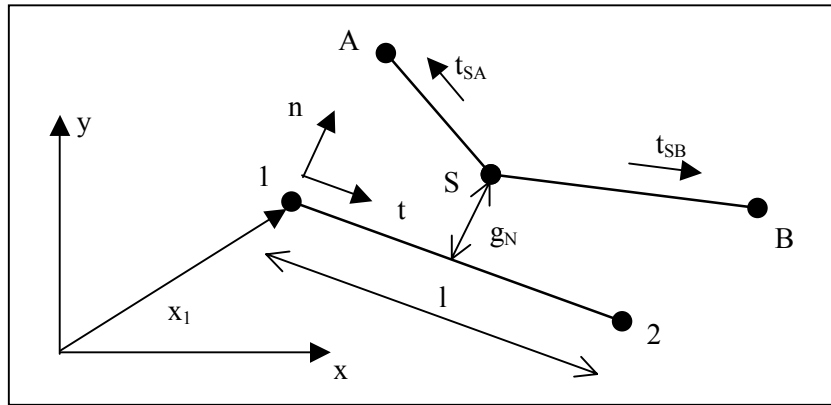


Figure 1. Contact element geometry

The electric field requires the definition of the contact voltage jump g_V

$$g_V = V_S - (1 - \xi)V_1 - \xi V_2 \quad (14)$$

where V_S , V_1 and V_2 are the electric potential of nodes S, 1 and 2, while ξ is the distance between the master node 1 and the projection of the slave node S onto the segment 12, normalized to the segment length $\xi = \frac{1}{l}(\mathbf{x}_S - \mathbf{x}_1) \cdot \mathbf{t}$.

The element pointwise penetration check requires a pointwise force balance. Since the physical laws are formulated with dependence on the contact pressure the definition of the contact area is required

$$A = \frac{1}{2}(\|\mathbf{x}_S - \mathbf{x}_A\| + \|\mathbf{x}_S - \mathbf{x}_B\|)s \quad (15)$$

where s is the depth of the contact element.

3.2. Normal and electric contact stiffness

To develop the constitutive law the mean planes distance, d , is replaced by the difference between the maximum asperities height ζ and the normal gap g_N , i.e. $d = \zeta - g_N$. The normal force F_N is finally obtained as a product of the apparent contact area and the apparent pressure. Recalling eq. (8)

$$F_N = A_a \frac{c_1}{2} \left[4 \cdot 10^6 \frac{\sigma}{m} \right]^{c_2} \exp \left[\left(\frac{c_2}{2\sigma^2} \right) (\zeta - g_N)^2 \right] \left[\operatorname{erfc} \left(\frac{(\zeta - g_N)}{\sqrt{2}\sigma} \right) \right]^{1+c_2} \quad (16)$$

Collecting numerical constants and constant parameters in a suitable form

$$K_{NP} = \frac{c_1}{2} \left(\frac{2}{\sqrt{\pi}} \right)^{1+c_2} \left[4 \cdot 10^6 \frac{\sigma}{m} \right]^{c_2}; \quad c_3 = \frac{c_2}{2\sigma^2} \quad (17)$$

Equation (16) can be written as

$$F_N = A_a K_{NP} \exp \left[c_3 (\zeta - g_N)^2 \right] \left[\int_{\frac{\zeta - g_N}{\sqrt{2}\sigma}}^{\infty} e^{-y^2} dy \right]^{1+c_2} = f(A_a, g_N) \quad (18)$$

The final form of the constitutive law for normal contact depends upon the normal gap and the apparent contact area. In this form the normal force can easily be expressed as a function of the unknown nodal displacements after the Finite Element discretisation.

Substituting equation (7) and (8) in eq. (12) we obtain the exact formulation for the expression of the electric current

$$I = A_a h_V g_V = A_a K_{NV} \left[\left(1 - \sqrt{\frac{1}{2} \operatorname{erfc}\left(\frac{\zeta - g_N}{\sqrt{2}\sigma}\right)} \right)^{-3/2} \exp\left(\frac{-(\zeta - g_N)^2}{2 \cdot \sigma^2}\right) \right] g_V \quad (19)$$

$$= f(A_a, g_N, g_V)$$

Also in this case the relationship is formulated as a function of the apparent contact area, the normal gap and the voltage jump, i.e. as a function of terms than can be easily expressed in terms of the primary variables.

3.3. Global equation set

The contact element contribution to the global tangent stiffness matrix can be computed by adding to the variation of a known functional $\bar{\Pi}$ - representing the continuum - the virtual work given by the contact force and the analogous quantities in the electric field

$$\delta_u(\Pi_M) = \delta_u(\bar{\Pi}_M(u, V)) + \bigcup_{active} [F_N \cdot \delta_u g_N] = 0$$

$$\delta_V(\Pi_E) = \delta_V(\bar{\Pi}_E(V, u)) + \bigcup_{active} [I \cdot \delta_V g_V] = 0 \quad (20)$$

The linearization of the system (20), taking into account all the possible dependences and coupling terms generates a complex form with several terms, some of which are discussed in detail in [12]. The contributions have different importance, and some of them may be disregarded or vanish. At present the most important terms have been implemented in the code, they are collected in the following expressions, evidencing the purely mechanical and purely electric contributions as well as the coupling terms

Mechanical contribution of the contact elements

$$\bigcup \left[\frac{\partial F_N}{\partial g_N} \cdot \Delta_u g_N \delta_u g_N + \frac{\partial F_N}{\partial A} \cdot \Delta_u A \delta_u g_N + F_N \cdot \Delta_u \delta_u g_N \right]$$

Electric contribution of the contact elements

$$\bigcup \left[\frac{\partial I}{\partial g_V} \cdot \Delta_V g_V \delta_V g_V \right] \quad (21)$$

Coupling terms

$$\bigcup \left[\frac{\partial I}{\partial A} \cdot \Delta_u A \delta_V g_V + \frac{\partial I}{\partial g_N} \cdot \Delta_u g_N \delta_V g_V + \frac{\partial I}{\partial g_V} \cdot \Delta_u g_V \delta_V g_V + I \cdot \Delta_u \delta_V g_V \right]$$

Virtual and finite variations of geometric parameters are involved in equations (21). In order to achieve a good computational efficiency consistent linearization of the terms is developed, details can be found in [11-12] for the geometrical terms and in [7] for the electric-mechanical contributions. Here the variations will be directly expressed in matrix form.

3.4. Matrix notation

We need the definition of some auxiliary vectors in order to express the stiffness terms in a suitable form for the Finite Element technique. For this purpose geometrical parameters can be combined in suitable vectors

$$\mathbf{N}_S = \begin{bmatrix} \mathbf{n} \\ -(1-\xi) \cdot \mathbf{n} \\ -\xi \cdot \mathbf{n} \end{bmatrix} \quad \mathbf{T}_S = \begin{bmatrix} \mathbf{t} \\ -(1-\xi) \cdot \mathbf{t} \\ -\xi \cdot \mathbf{t} \end{bmatrix} \quad \mathbf{N}_0 = \begin{bmatrix} \mathbf{0} \\ -\mathbf{n} \\ \mathbf{n} \end{bmatrix} \quad (22a)$$

$$\mathbf{T}_{GS} = \frac{1}{2} \begin{bmatrix} -\mathbf{t}_{SA} - \mathbf{t}_{SB} \\ \mathbf{0} \\ \mathbf{0} \end{bmatrix} \quad \mathbf{T}_{GAB} = \frac{1}{2} \begin{bmatrix} \mathbf{0} \\ \mathbf{t}_{SA} \\ \mathbf{t}_{SB} \end{bmatrix} \quad (22b)$$

$$\mathbf{G}_M = \begin{bmatrix} 1 \\ -(1-\xi) \\ -\xi \end{bmatrix} \quad \mathbf{U} = \begin{bmatrix} 0 \\ 1 \\ -1 \end{bmatrix} \quad (22c)$$

If we order the unknowns collecting respectively the mechanical degrees of freedom of nodes S, 1, 2, A and B and then electric degrees of freedom of node S, 1 and 2, the consistent stiffness matrix can be written as

$$[\mathbf{K}_T]_{13 \times 13} = \begin{bmatrix} \mathbf{K}_{TMecc} & \mathbf{K}_{TMeccAB} & \mathbf{0} \\ \mathbf{0} & \mathbf{0} & \mathbf{0} \\ \mathbf{K}_{TCouplS12} & \mathbf{K}_{TElecAB} & \mathbf{K}_{TElec} \end{bmatrix} \quad (23)$$

where \mathbf{K}_{TMecc} and \mathbf{K}_{TElec} are sub-matrixes expressing the purely mechanical and purely electric contributions respectively, while $\mathbf{K}_{TMeccAB}$, $\mathbf{K}_{TElecAB}$ represent the dependence of the mechanical and electric field on the variation of the element area. The sub-matrix $\mathbf{K}_{TCouplS12}$ is the coupling sub-matrix between the electric resistance and the normal gap.

In detail we have

$$\mathbf{K}_{TMecc} = \frac{\partial F_N}{\partial g_N} \mathbf{N}_S \cdot \mathbf{N}_S^T - \frac{F_N}{l} \left[\mathbf{N}_0 \cdot \mathbf{T}_S^T + \frac{g_N}{l} \cdot \mathbf{N}_0 \cdot \mathbf{N}_0^T + \mathbf{T}_S \cdot \mathbf{N}_0^T \right] + \frac{\partial F_N}{\partial A_a} \mathbf{N}_S \cdot \mathbf{T}_{GS}^T \quad (24)$$

$$\mathbf{K}_{TElec} = \frac{\partial I}{\partial g_V} \mathbf{G}_M \cdot \mathbf{G}_M^T \quad (25)$$

$$\mathbf{K}_{TMeccAB} = \frac{\partial F_N}{\partial A_a} \mathbf{N}_S \cdot \mathbf{T}_{GAB}^T \quad \mathbf{K}_{TElecAB} = \frac{\partial I}{\partial A_a} \mathbf{G}_M \cdot \mathbf{T}_{GAB}^T \quad (26)$$

$$\begin{aligned} \mathbf{K}_{TCouplS12} = & \frac{\partial I}{\partial \mathbf{g}_N} \mathbf{G}_M \cdot \mathbf{N}_S^T + \frac{\partial I}{\partial \mathbf{g}_V} \frac{(V_1 - V_2)}{l} \cdot \left[\mathbf{G}_M \cdot \mathbf{T}_S^T + \frac{\mathbf{g}_N}{l} \mathbf{G}_M \cdot \mathbf{N}_0^T \right] + \\ & \frac{I}{l} \mathbf{U} \cdot \left[\mathbf{T}_S^T + \frac{\mathbf{g}_N}{l} \mathbf{N}_0^T \right] + \frac{\partial I}{\partial A_a} \mathbf{G}_M \cdot \mathbf{T}_{GS}^T \end{aligned} \quad (27)$$

4. CONCLUDING REMARKS

The problem of contact in the coupled electric-mechanical field is developed in detail and a new 2D electric-mechanical contact element is derived. It can be effectively used to study a wide range of problems in the electric-mechanical field with a good degree of precision. Contact constraints are incorporated into the virtual work equations using the penalty method, the global equation set is obtained and the electric, mechanical and coupling terms are expressed in suitable matrix form easy to implement in a Finite Element code.

The preliminary practical applications show very satisfactory results, the effective validation of the numerical formulation is now in progress and will be dealt with in a succeeding paper.

REFERENCES

- [1] Cooper M. G., Mikic B. B., Yovanovich M. M., Thermal contact conductance, *Int. J. of Heat and Mass Transfer*, Vol. 12, pp. 279-300 (1969).
- [2] Mikic B. B., Analytical studies of contact of nominally flat surfaces; effect of previous loading, *Journal of Lubrication Technology*, Vol. 93, pp. 451-459 (1971).
- [3] Mikic B. B., Thermal Contact Conductance; Theoretical Considerations, *Int. J. of Heat and Mass Transfer*, Vol. 17, pp. 205-214 (1974).
- [4] Yovanovich M. M., Thermal Contact Correlation, *AIAA Paper*, pp. 83-95 (1981).
- [5] Song S., Yovanovich M. M., Explicit Relative Contact Pressure Expression: Dependence Upon Surface Roughness Parameters and Vickers Microhardness Coefficients, *AIAA 25th Aerospace Sciences Meeting*, Reno Nevada (1987).
- [6] Zavarise G., Boso D., Schrefler B. A., A contact formulation for electrical and mechanical contact resistance, *CMIS - 3rd Contact Mechanics International Symposium*, Peniche (Lisbon), Portugal, June 17-21, 2001.
- [7] Boso D. P., Schrefler B. A. Zavarise G., A coupled electric-mechanical approach for contact problems, accepted for *WCCM V Fifth World Congress on Computational Mechanics*, Vienna, Austria, 2002.
- [8] Hegazy A. H., Thermal joint conductances of conforming rough surfaces: effects of surface microhardness variation, PhD Thesis, Dept. of Mechanical Engineering, University of Waterloo, Canada (1985).
- [9] Holm R., *Electric Contacts: Theory and applications*, 4th edn., Springer Verlag, Berlin Heidelberg New York (1981).
- [10] P. Wriggers, J. C. Simo, A note on tangent stiffness for fully nonlinear contact problems, *Comm. Appl. Numer. Meth.*, Vol. 1, pp. 199-203 (1985).
- [11] G. Zavarise, P. Wriggers, E. Stein, B. A. Schrefler, Real contact mechanisms and finite element formulation – A coupled thermomechanical approach, *Int. J. Num. Meth. Eng.*, pp. 767-785 (1992).
- [12] B. A. Schrefler, G. Zavarise, Constitutive laws for normal stiffness and thermal resistance of a contact element, *Microcomp. Civ. Eng.*, Vol. 8, pp 299-308 (1993).